Land Surface Temperature Retrieval of Landsat-8 Data Using Split Window Algorithm-A Case Study of Mosul District

Amal Muhammad Saleh

College of Agriculture /University of Baghdad
geetakh@gmail.com

Abstract: The main purpose of this paper is to present an operational algorithm to retrieve the Land Surface Temperature (LST) and Land Surface Emissivity (LSE) in Mosul District, Ninawa Province, Iraq from Landsat-8 data of September 16, 2015. The proposed algorithm is Split-Window (SW) with brightness temperature value of both band 10 (10.60 - 11.19μm) and band 11 (11.50 - 12.51 μm) of Landsat-8 in thermal infrared range. Normalized Difference Vegetation (NDVI) threshold values have been determined to separate the bare soil, and vegetated areas from each other. Fractional Vegetation Cover (FVC) was derived with the help of NDVI threshold technique. Emissivity values of bands 10 and 11 are calculated through FVC. The results showed that the spatial variation of land surface temperature was more reliable and accurate in entire Mosul District.
[Amal Muhammad Saleh. **Land Surface Temperature Retrieval of Landsat-8 Data Using Split Window Algorithm-A Case Study of Mosul District.** *J Am Sci* 2017;13(12):62-75]. ISSN 1545-1003 (print); ISSN 2375-7264 (online). http://www.jofamericanscience.org. 8. doi:10.7537/marsjas131217.08.

Keywords: Land Surface Temperature; Land Surface Emissivity; Fractional Vegetation Cover; Split-Window; NDVI.

1. Introduction

Land surface temperature (LST) is one of the most important parameters in the physical processes of surface energy and water balance at local through global scales (Karnieli et al., 2010). Knowledge of the LST provides information on the temporal and spatial variations of the surface equilibrium state and is of fundamental importance in many applications (Kerr et al., 2000). As such, the LST is widely used in a variety of fields including evapotranspiration, climate change, hydrological cycle, vegetation monitoring, urban climate and environmental studies, among others (Hansen et al., 2010). and has been recognized as one of the high-priority parameters of the International Geosphere and Biosphere Program (IGBP) (Townshend et al., 1994). Due to the strong heterogeneity of land surface characteristics such as vegetation, topography, and soil, LST changes rapidly in space as well as in time and an adequate characterization of LST distribution and its temporal evolution, therefore, requires measurements with detailed spatial and temporal sampling (Neteler, 2010).

Given the complexity of surface temperature over land, ground measurements cannot practically provide values over wide areas. With the development of remote sensing from space, satellite data offer the only possibility for measuring LST over the entire globe with sufficiently high temporal resolution and with complete spatially averaged rather than point values. (Li et al., 2013).

The major objectives of the study are to find the brightness temperature using band 10 and band 11 of TIR, calculate the LSE using NDVI threshold technique and estimate the LST of Mosul District using Split-Window (SW) algorithm.

2. Material and Methods

Mosul is a city in northern Iraq Located some 400 km (250 mi) north of Baghdad, the original city stands on the west bank of the Tigris River, opposite the ancient Assyrian city of Nineveh on the east bank (Figure 1a). It is geographically situated on latitude 35º 33′ 54.67″-36º 32′ 03.79″ North and longitude 42º 43′ 12.46″ - 43º 03′ 21.78″ East. Mosul experiences a hot semi-arid climate (Köppen climate classification BSh) (Peel et al., 2007). The winter is mild, but certainly it's not tropical; the January average is 7 °C. The summer in Mosul is very hot, with a relentless sun, and with daytime temperatures of 43°C in July and August, but with peaks of 47/48°C; however, the relative humidity is between 25% - 79% (Brugge, 2014). Mosul is at an altitude of about 228 metres (748ft) above sea level. Throughout the year, in Mosul, 365 mm of rain fall: they are not many, but they are concentrated between November and April, with very few rains in May and October, while between June and September it almost never rains (Dessler and Parson, 2006). The average annual wind speed of Mosul is 1.26 m/s, (Hassoon, 2013).

Landsat 8 is one of the Landsat series of NASA. The data of Landsat 8 is available in Earth Explorer website at free of cost. In the present study, the TIR bands 10 and 11 were used to estimate brightness temperature and OLI spectral bands 2, 3, 4, and 5 were used to generate NDVI of the study area (Figure

1b), (Table 1). Landsat 8 provides metadata of the bands such as thermal constant, rescaling factor value etc., which can be used for calculating various algorithms like LST.

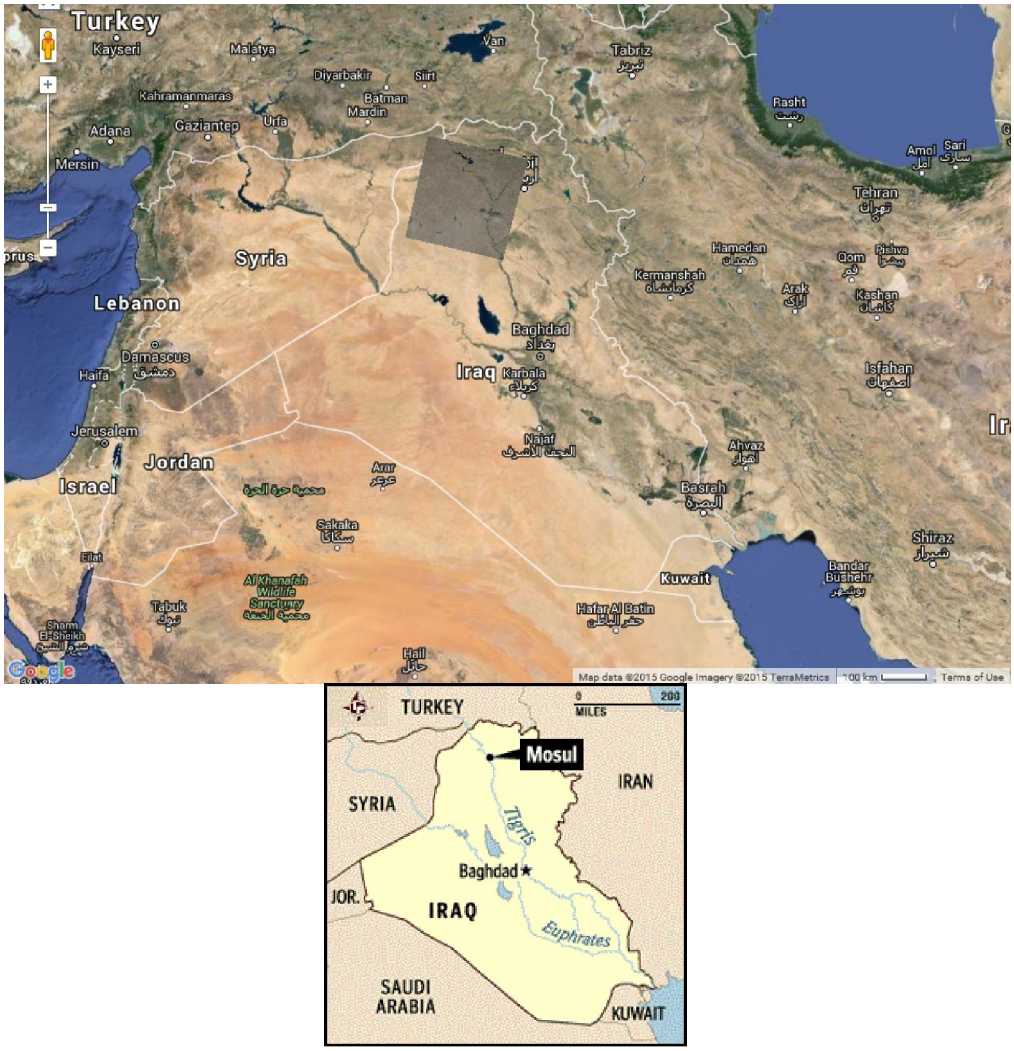

Figure 1. (a) Location map of the study area, (b) The Satellite Landsat OLI and TIRS scene.

The value of Top of Atmospheric (TOA) spectral radiance (L_λ) was determined by multiplying multiplicative rescaling factor (0.0003342) of TIR bands with its corresponding TIR bands and adding additive rescaling factor (0.1) with it (Table 2).

$$L_\lambda = ML * Qcal + AL \quad (1)$$

Where:

L_λ - Top of Atmospheric Radiance in watts/(m^2 * srad * μm).

M_L - Band specific multiplicative rescaling factor (radiance_mult_band_10/11).

Qcal - band 10/ 11 image.

A_L - Band specific additive rescaling factor (radiance_add_band_10/11).

Estimation of Brightness Temperature (T_B) of Band 10 and 11 is the electromagnetic radiation traveling upward from the top of the Earth's atmosphere. Thermal calibration process has been done by converting thermal DN values of raw thermal bands of TIR sensor into Top of Atmospheric (TOA) Spectral Radiance.

Using ERDAS IMAGINE 9.2 Modeler we implement algorithm of equation-2.

$$T_B = \frac{K2}{Ln\left(\frac{K1}{L\lambda}+1\right)} \quad (2)$$

Where:

T_B - Brightness Temperature.

L_λ - Top of Atmospheric spectral radiance in watts/

(m^2 * srad * μm).

K_1 and K_2 - Band-specific thermal conversion constant from the metadata image file and it varies for both TIR bands (Table 3).

OLI bands 2, 3, 4 and 5 were layer stacked and NDVI was calculated using algorithm shown in equation-3 (Rouse et al., 1974).

$$NDVI = \frac{BAND_5 - BAND_4}{BAND_5 + BAND_4} \quad (3)$$

Range: -1 < NDVI < + 1

Where:

NDVI - Normalized Difference Vegetation Index.

BAND4 - TOA planetary reflectance values from Red band.

BAND5 - TOA planetary reflectance values from Near Infrared band.

The relationship between LST and NDVI takes into account that vegetation and soils are the main surface cover for the terrestrial component (Snyder et al., 1998).

Table 1. Metadata of Satellite Image.

OLI	Reflective (8)	30.00	170 / 035	16 September 2015

Table 2. Radiometric rescaling Factor.

Table 3. Thermal constant values.

Estimation of Fractional Vegetation Cover (FVC) was implemented using NDVI image. Fractional Vegetation Cover estimate the fraction of an area under vegetation. Split-Window algorithm utilize FVC to estimate Land Surface Emissivity (LSE). Using ARC MAP 10.3 we reclassify the NDVI layer into soil and vegetation and calculate NDVI for Soil and Vegetation (Table 4).

Table 4. NDVI for Soil and Vegetation.

NDVI for Soil	0.060304167

Using ERDAS IMAGINE 9.2 Modeler we calculated the algorithm of FVC of equation-4 (Carlson and Ripley, 1997; Gutman and Ignatov, 1998).

$$FVC = \frac{NDVI - NDVI_S}{NDVI_V - NDVI_S} \quad (4)$$

Where:

FVC - Fractional Vegetation Cover.

NDVIs - NDVI reclassified for soil.

NDVIv - NDVI reclassified for vegetation.

The correct determination of the surface temperature is constrained to an accurate knowledge of surface emissivity. The emissivity of a surface is controlled by such factors as water content, chemical composition, structure and roughness. It can be determined as the contribution of the different components that belong to the pixels according to their proportions (Snyder et al., 1998).

Estimation of Land Surface Emissivity (LSE) was obtained from FVC layer. Land Surface Emissivity measure the inherent characteristic of earth surface. LSE estimation required emissivity of soil and vegetation of both Band 10 and 11 (Table 5).

Table 5. Emissivity values.

Emissivity	Band 10	Band 11
ε_s	0.971	0.977

[Source: Skoković et al., 2014]

LSE of Band 10 and 11 were individually calculated as shown in equation-5.

$$LSE = \varepsilon_s * (1 - FVC) + \varepsilon_v * FVC \quad (5)$$

Where:

LSE - Land Surface Emissivity.

ε_s - Emissivity for soil.

ε_v - Emissivity for vegetation.

FVC - Fractional Vegetation Cover.

Combination of LSE of Band 10 and LSE of Band 11 was obtained through Mean and Difference

between them as shown in equation-6 & 7 (Sobrino et al., 1996).

$$m = \frac{LSE_{10} + LSE_{11}}{2} \quad (6)$$

$$\Delta m = LSE_{10} - LSE_{11} \quad (7)$$

Where:

m - Mean of LSE.

LSE_{10} - LSE of band 10.

LSE_{11} - LSE of band 11.

Δm - Difference of LSE

Land Surface Temperature (LST) was calculated by applying a structured mathematical algorithm viz., Split-Window (SW) algorithm. It uses brightness temperature of two bands of TIR, mean and difference in land surface emissivity for estimating LST of an area. Using ERDAS IMAGINE 9.2 Modeler we implement the algorithm of equation-8.

$$LST = TB_{10} + C_1 (TB_{10} - TB_{11}) + C_2 (TB_{10} - TB_{11})^2 + C_0 + (C_3 + C_4 W)(1-m) + (C_5 + C_6 W)\Delta m \quad (8)$$

Where:

LST - Land Surface Temperature (K°).

TB_{10} and TB_{11} - Brightness Temperature of band 10 and band 11 (K°).

C_0 To C_6 - Split-Window Coefficient values (Table 6).

m - mean LSE of TIR bands.

Δm - Difference of LSE.

W- Atmospheric water-vapour content =14.215 g/cm^2 [Source: Iraqi Meteorological Organization And Seismology, 2015].

Table 6. Split-Window coefficient values.

Constant	Value
C_0	-0.268
C_1	1.378
C_2	0.183
C_3	54.300
C_4	-2.238
C_5	-129.200
C_6	16.400

[Source: Skoković et al., 2014]

3. Results

NDVI map revealed that the NDVI value varies between -0.0923236 to 0.557708. Healthy and green vegetation cover area had highest NDVI value whereas area under water body had negative value (Figure 2). The NDVI value of area under vegetation was more than 0.060304167 and for built-up and barren land was 0 - 0.060304167. We calculate Fractional vegetation cover (FVC) using equation-4 as shown in Figure (3) and LSE using equation-5.

We implement algorithm in ERDAS IMAGINE 9.2 Modeler to calculate difference and mean LSE Layer shown in Figure (4) and Figure (5). Mean LSE Layer of Mosul Province ranged between 0.969 - 0.988. Highly elevated regions in the Province had more vegetative cover, hence LSE was high in these regions.

We take TIRS band 10 and 11 to estimate Brightness Temperature (TB) in Kelvin using the algorithm of equation-2 shown in Figure (6) and Figure (7). From Figure (8) and Figure (9) of statistical graph, we observe that class 5 exhibit 28.90% of the total area at a temperature between 302.28 -315.60 K° from TB of Band 10 and also class 5 of TB of Band 11 exhibit maximum of 27.68% of total area at a temperature between 298.52-311.11K°.

Figure (10) represent the final LST layer of Mosul Province on 16th September 2015. Area statistics graph of LST layer in Figure (11) proof that, it divide into two major land surface temperature class of 1 and 4 with statistics of 28.97% of an area under foothill regions at a temperature less than 269.20 K° by class 1 and 30.66% of an area under healthy vegetation land cover at a temperature in between 311.54 - 334.64 K° by class 4. Water bodies exhibit 20.83% of the total area at a temperature in between 292.29 - 311.54 K° by class 3. Cultivable land exhibit 17.52% of the total area at a temperature in between 269.20 - 292.29 K° by class 2. Remain 2.02% of an area under barren land and wasteland exhibit an LST more than 334.64 K° by class 5.

Validation of LST is of crucial importance for estimating the accuracy of the products and understanding the potential and limitations of satellite observations of LST. Validation of LST was carried out using a direct comparison of satellite-derived LST with collocated and simultaneously acquired LST from ground-based on 16th September 2015 (Iraqi Meteorological Organization And Seismology, 2015). Figure (12) shows a Linear regression of estimated vs. actual LST, the small bias & RMSE and the high coefficient of determination R^2 demonstrate the excellent quality of the Satellite Application Facility. The cold outliers are assumed to be caused by undetected cloud contamination or instrument -related problems.

4. Discussions

LST and LSE are two significant parameters in global change studies, in estimating radiation budgets in heat balance studies and as a control index for climate models. Emissivity, is an indicator of land-cover type and resources, and also a necessary element in the calculation of Land surface temperature (LST) from remotely sensed data. For LSE mapping, Fractional Vegetation Cover (FVC) of optical bands of OLI sensor of Landsat 8 had been derived. Split-Window algorithm (SW) is a dynamic mathematical

tool, provide the (LST) information using brightness temperature of thermal bands of TIRS sensor and Land surface emissivity (LSE). The study clearly revealed that 30.66% of the total area are under vegetation land cover at a temperature of 311.54 - 334.64 Kº and other 28.97% of the total area are under hilly regions at a temperature less than 269.20 Kº. Therefore the results indicate that the proposed (SW) algorithm can be a suitable and robust method to retrieve the LST map from Landsat-8 satellite data.

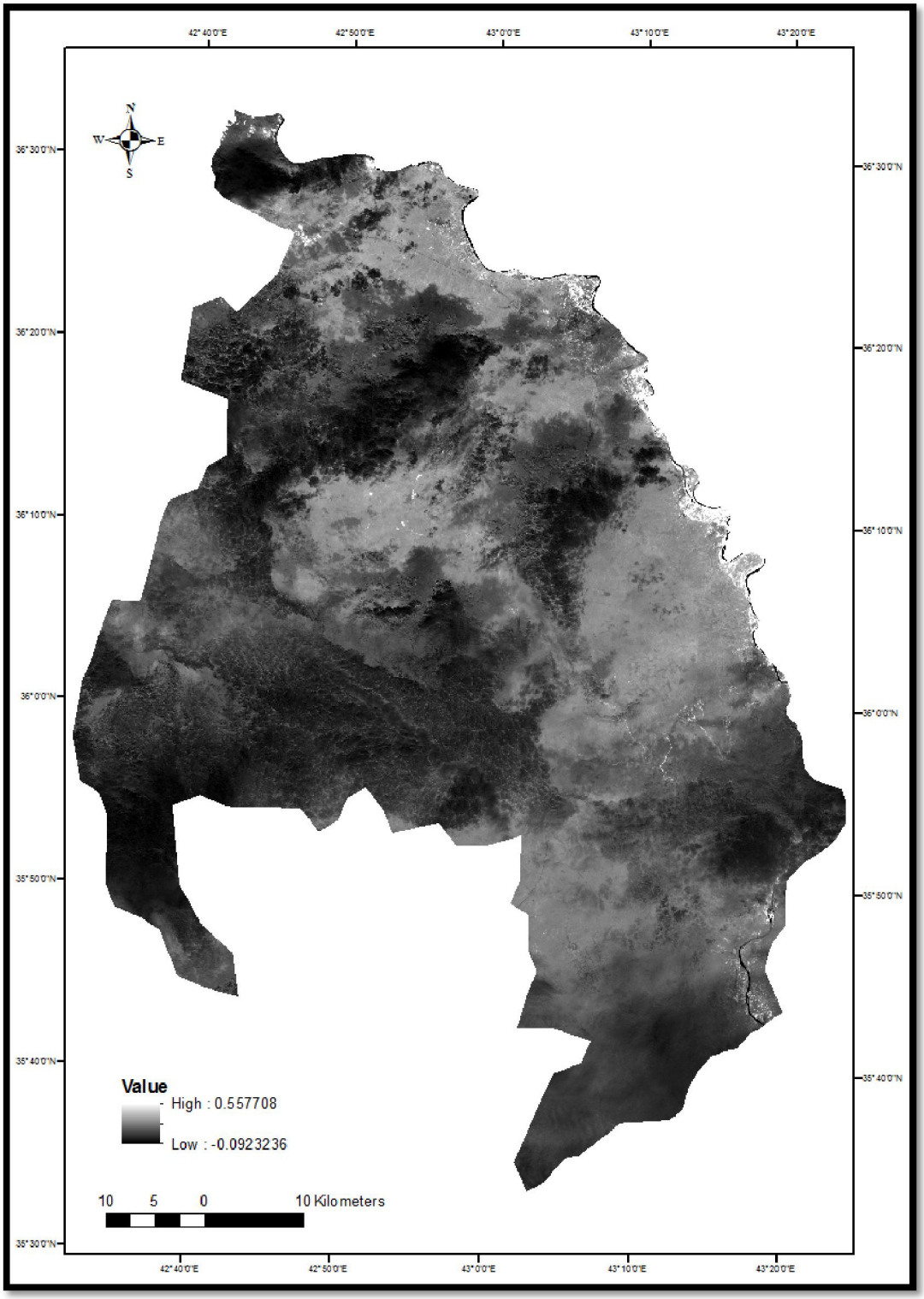

Figure 2. NDVI Layer of Mosul District on 16th September 2015.

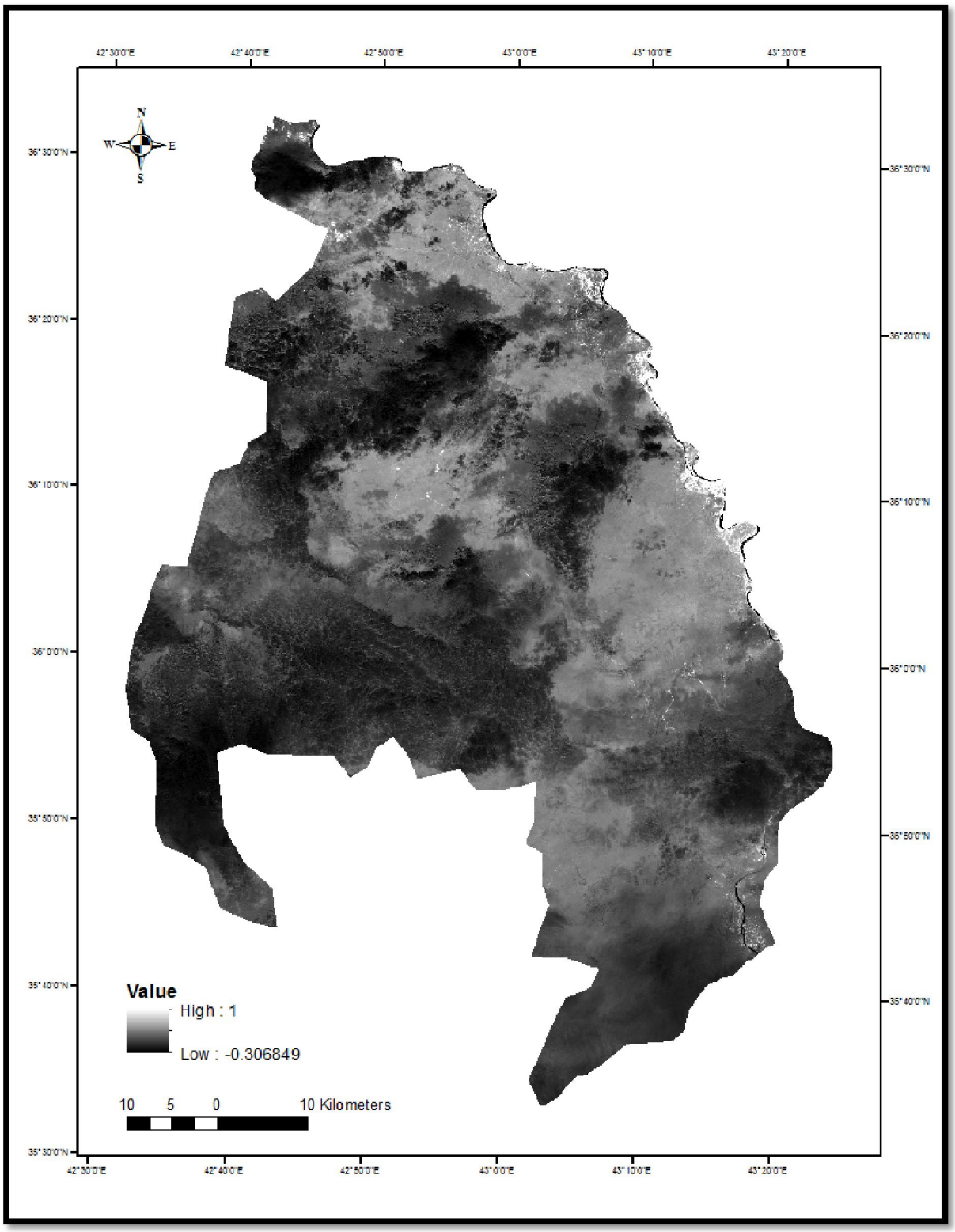

Figure 3. FVC Layer of Mosul District on 16th September 2015.

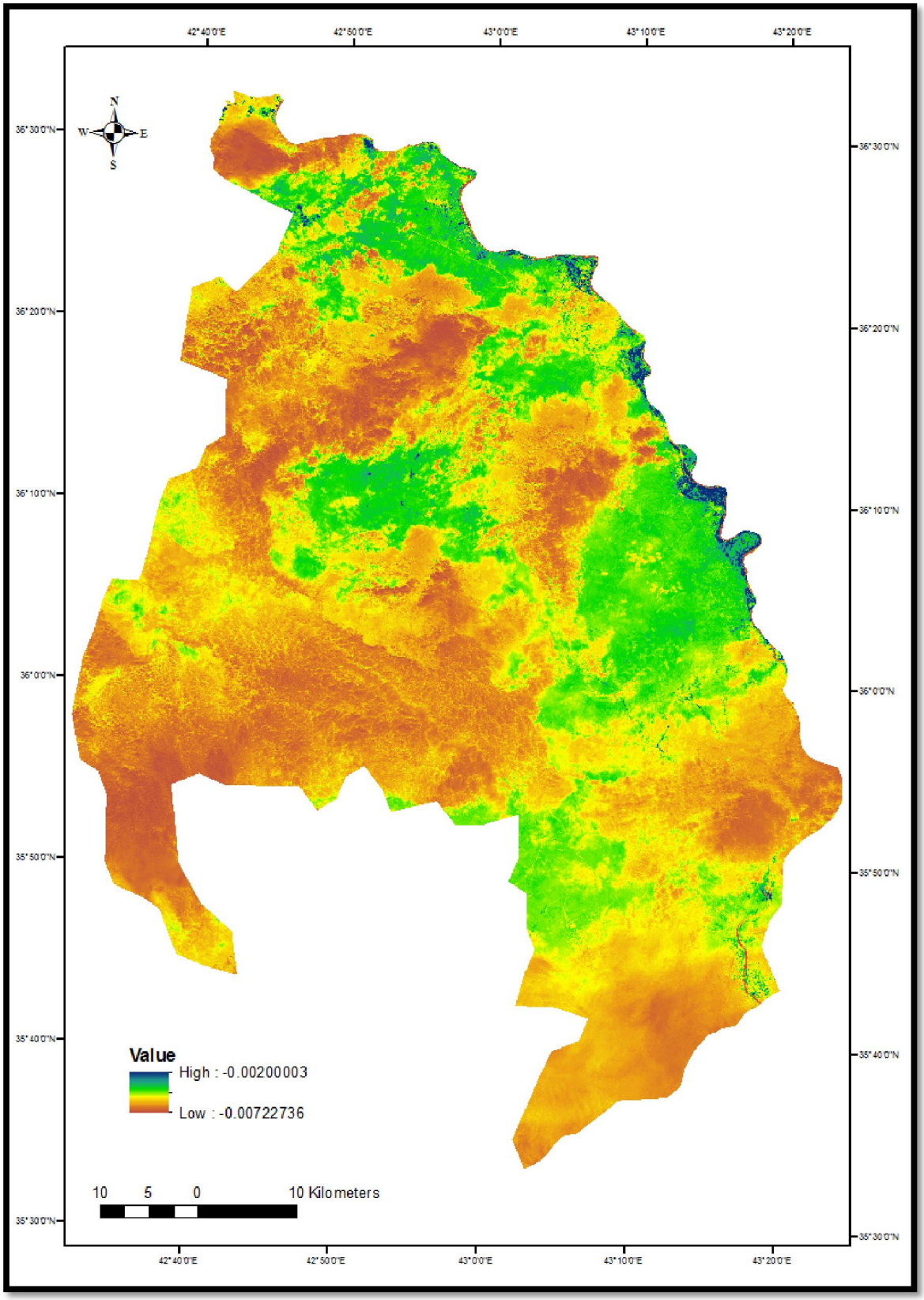

Figure 4. Difference LSE layer between Band 10 and 11.

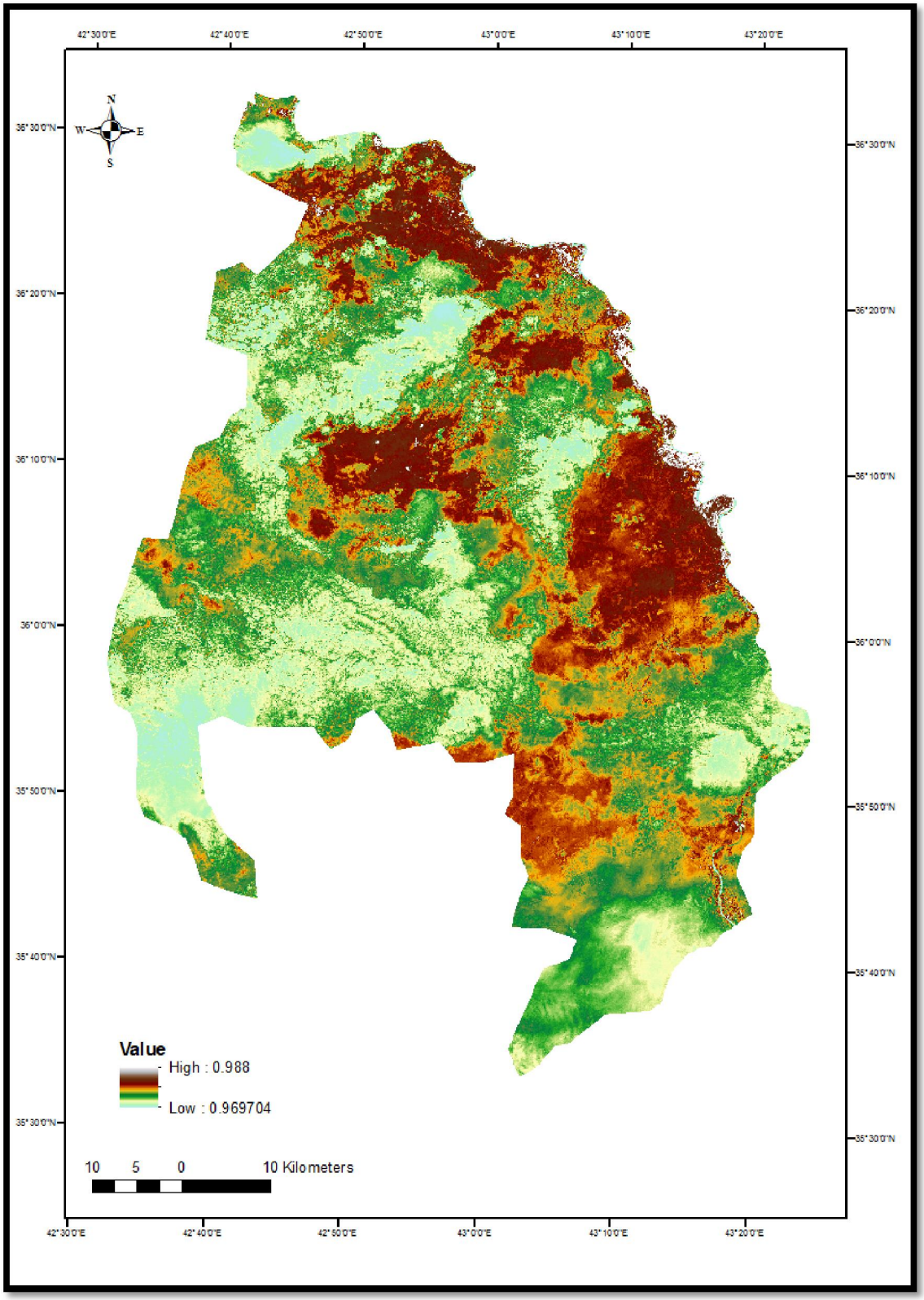

Figure 5. Mean of LSE layer between band 10 and 11.

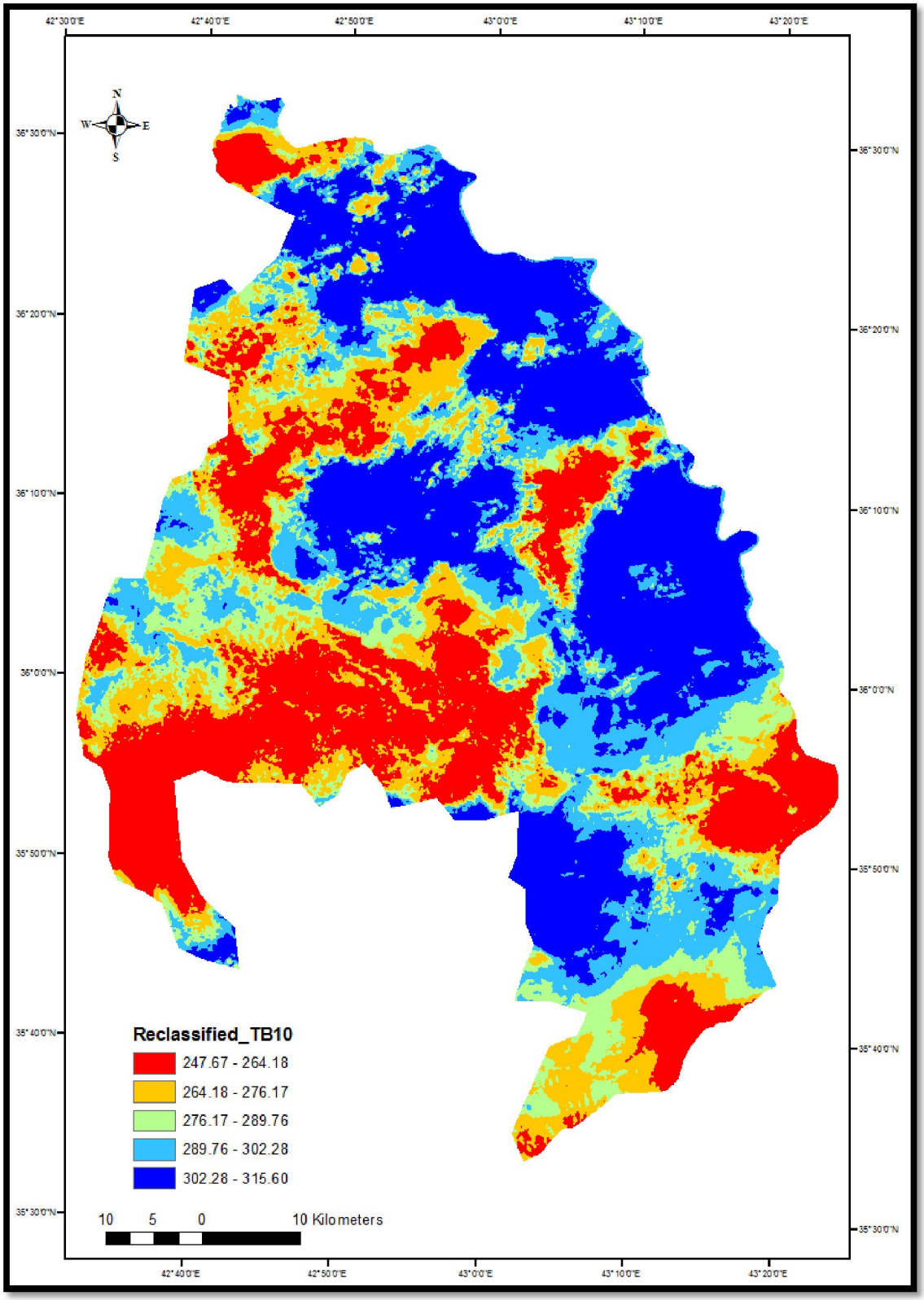

Figure 6. TB of Band 10 with label of Temperature intervals.

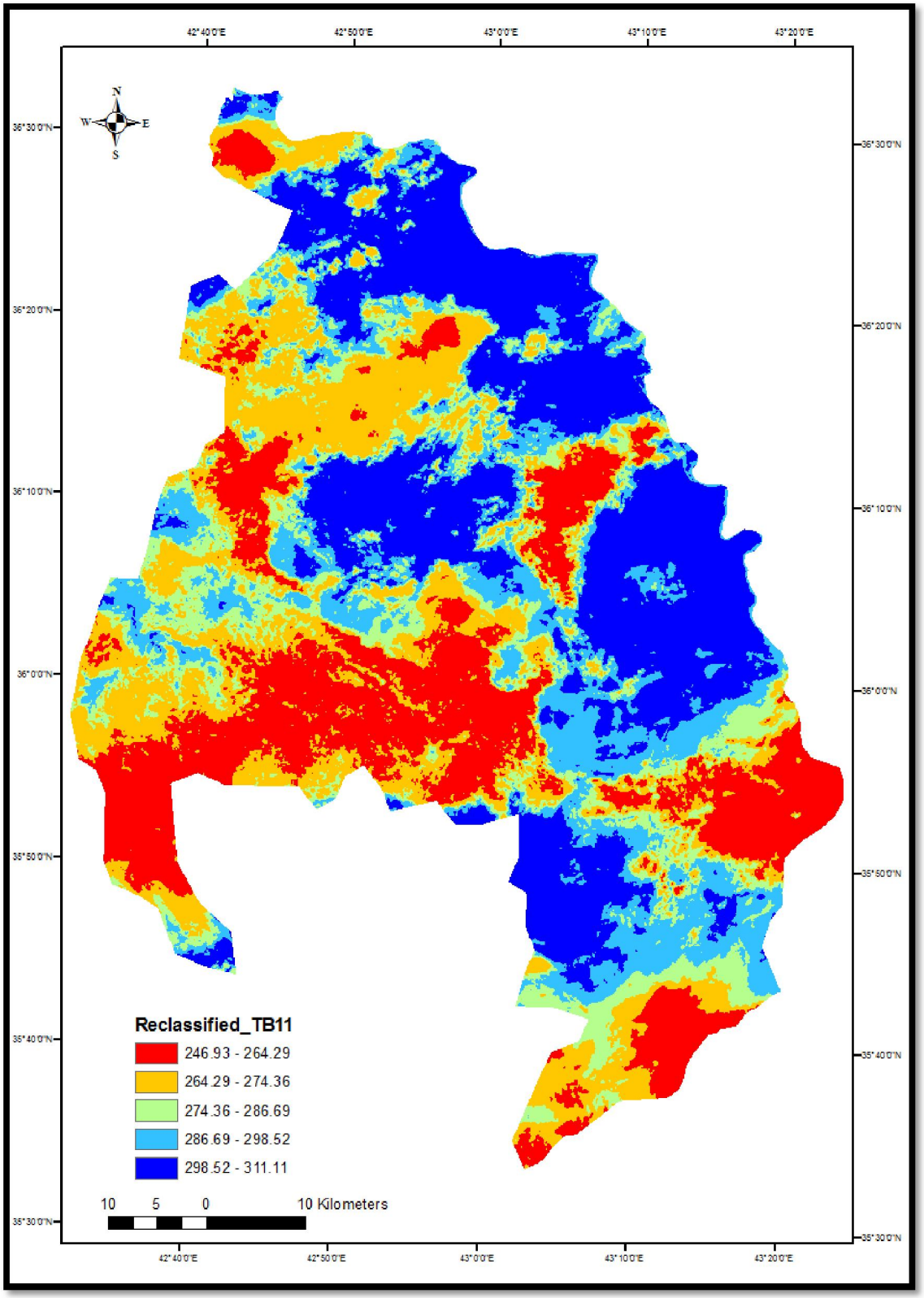

Figure 7. TB of Band 11 with label of Temperature intervals.

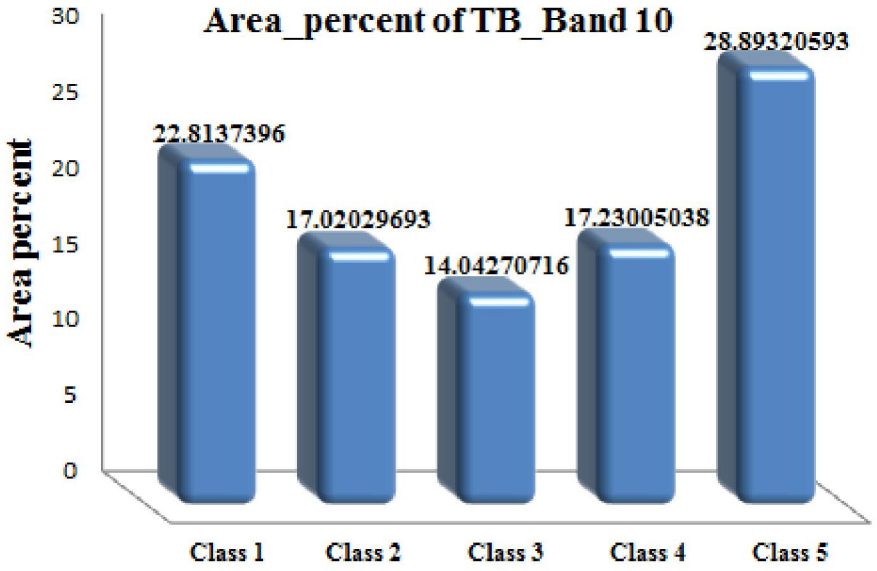

Figure 8. Area statistics of classified TB layer of Band 10.

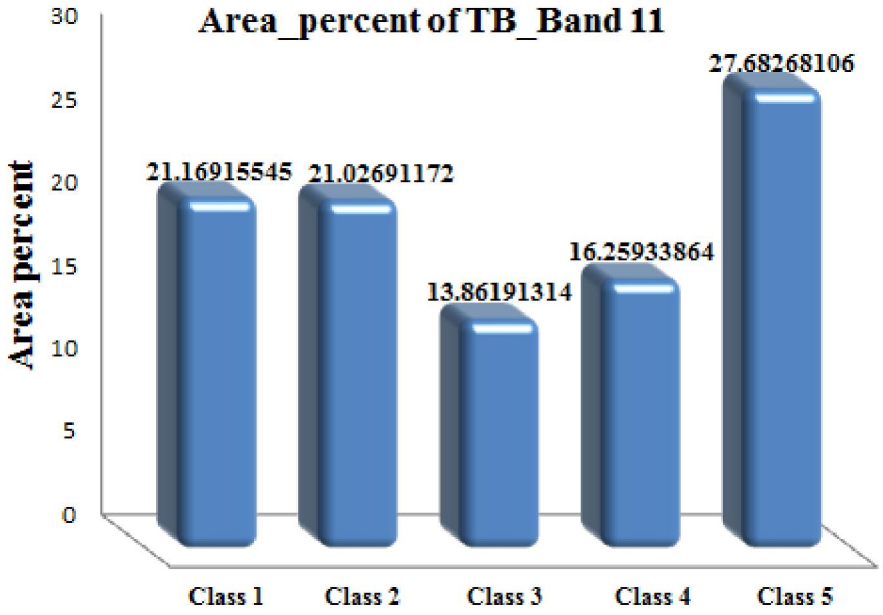

Figure 9. Area statistics of classified TB layer of Band 11.

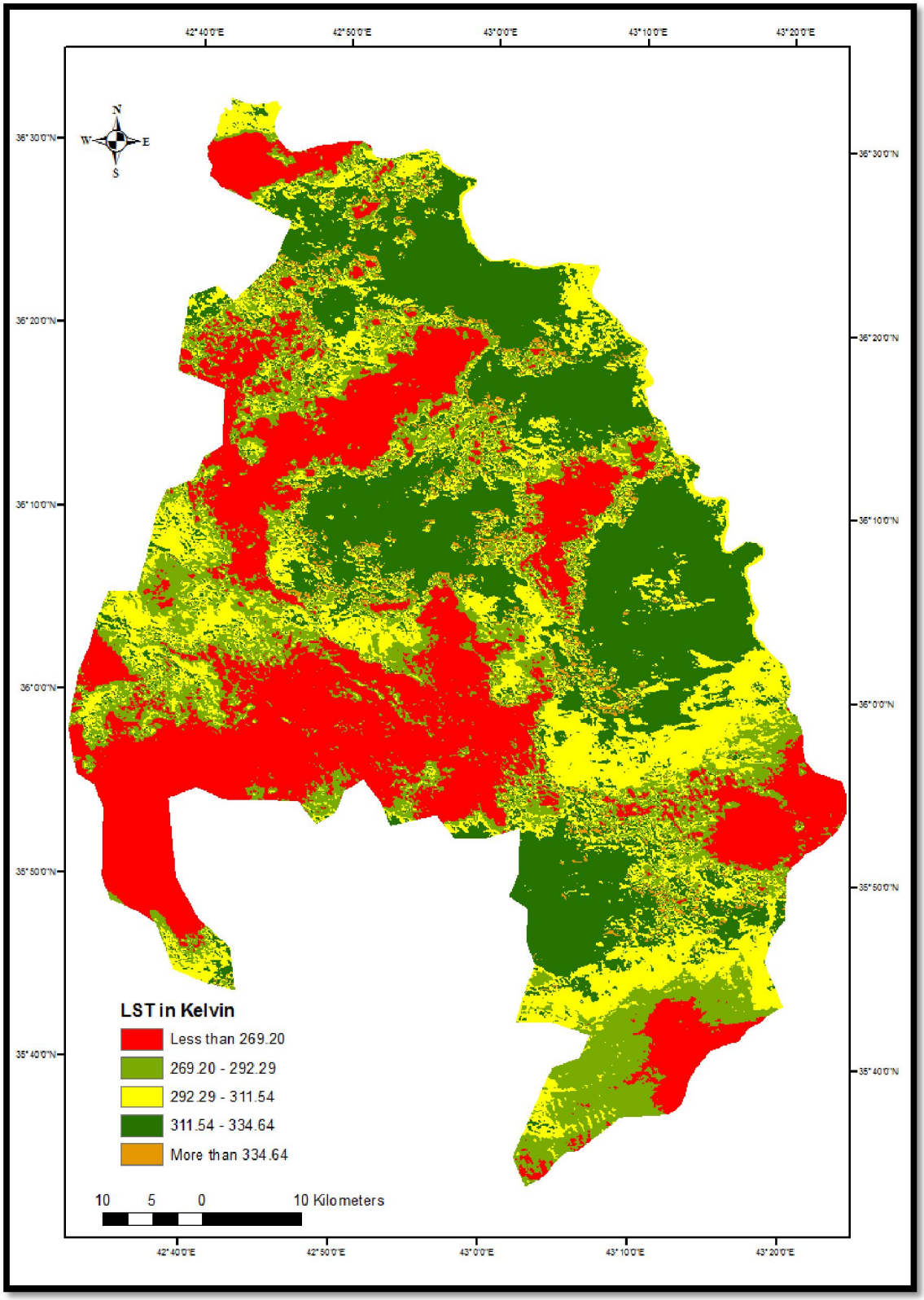

Figure 10. Land Surface Temperature Layer of Mosul District on 16th September 2015.

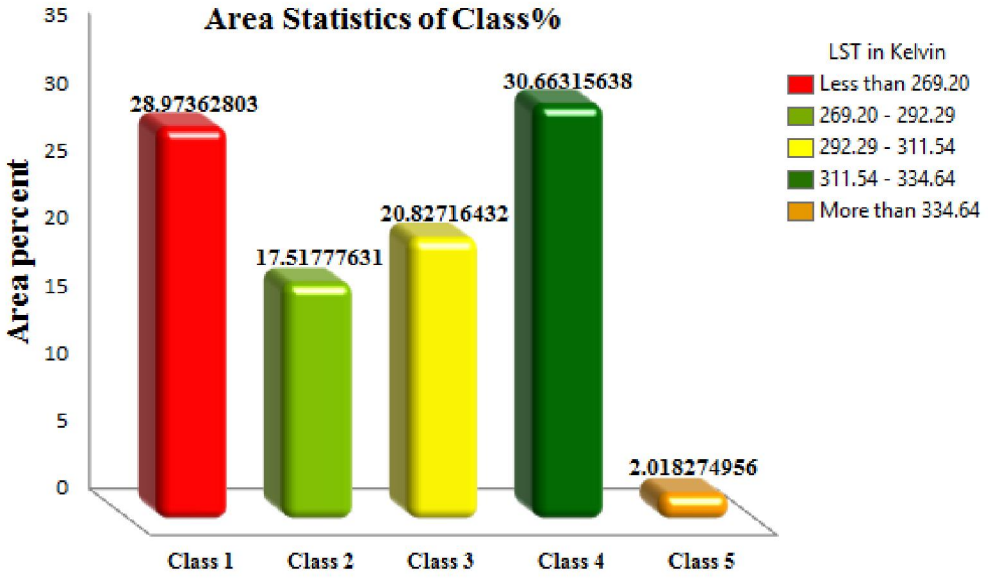

Figure 11. Graph of Area occupied (%).

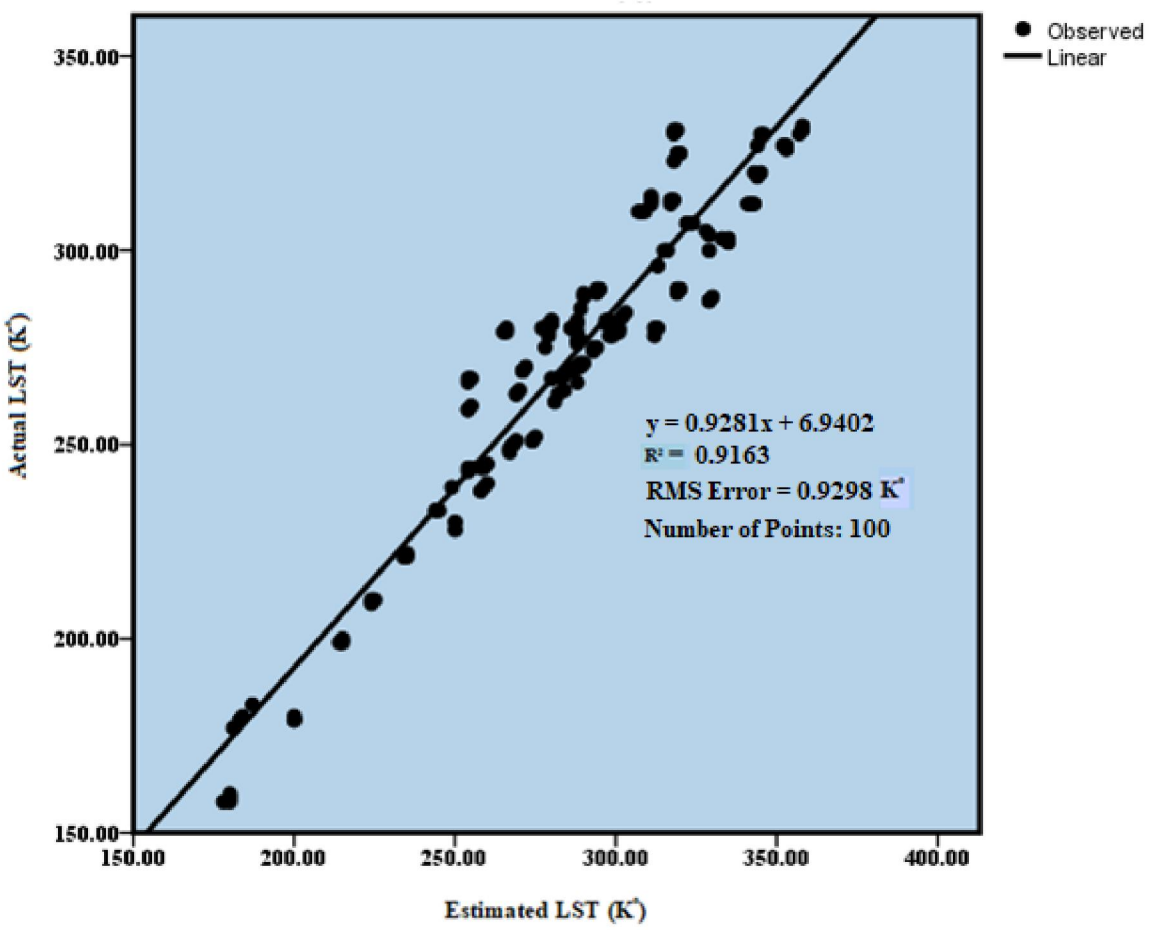

Figure 12. Scatter plot of estimated vs. actual LST.

Reference

1. Karnieli A, Agam N, Pinker RT, Anderson M, Imhoff ML, Gutman GG, Panov N, Goldberg A. Use of NDVI and land surface temperature for drought assessment: Merits and limitations. Journal of Climate 2010;23:633-618.
2. Kerr YH, Lagouarde JP, Nerry F, Ottlé C. Land surface temperature retrieval techniques and applications. In D. A. Quattrochi, & J. C. Luvall (Eds.), Thermal remote sensing in land surface processes, Boca Raton, Fla.: CRC Press, 2000:109-33.
3. Hansen J, Ruedy R, Sato M, Lo K. Global surface temperature change. Reviews of Geophysics 2010;48(4): RG4004.
4. Townshend JRG, Justice CO, Skole D, Malingreau JP, Cihlar J, Teillet P, Sadowski F, Ruttenberg S. The 1 km resolution global data set: needs of the International Geosphere Biosphere Programme. International Journal of Remote Sensing 1994;15(17):3441-3417.
5. Neteler M. Estimating daily land surface temperatures in mountainous environments by reconstructed MODIS LST Data. Remote Sensing 2010;2(1):351-333.
6. Li ZL, Tang B-H, Wu H, Ren H, Yan G, Wan Z, Trigo IF, Sobrino JA. Satellite-derived land surface temperature: Current status and perspectives. Remote Sensing of Environment 2013;131:37-14.
7. Peel MC, Finlayson BL, McMahon TA. Updated world map of the Köppen -Geiger climate classification. Hydrology and Earth System Sciences 2007;11:1644-1633.
8. Brugge R. World weather news, August 2011. Department of Meteorology, University of Reading, Archived from the original on 29 June 2014.
9. Hassoon AF. Determination trends and abnormal seasonal wind speed in Iraq. International Journal of Energy and Environment 2013;4(4):628-615.
10. Rouse JW, Haas RH, Schell JA, Deering DW. Monitoring vegetation systems in the Great Plains with ERTS. In Fraden S.C., Marcanti E.P. & Becker M.A. (eds.), Paper presented at the 3rd ERTS-1 Symposium, NASA SP-351, Washington D.C. NASA 1974a:317-309.
11. Snyder WC, Wan Z, Zhang Y, Feng YZ. Classification based emissivity for land surface temperature measurement from space, International Journal of Remote Sensing 1998;19(14):2774-2753.
12. Carlson TN, Ripley DA. On the relation between NDVI, fractional vegetation cover, and leaf area index. Remote Sensing of Environment 1997;62(3):252-241.
13. Gutman G, Ignatov A. The derivation of the green vegetation fraction from NOAA/AVHRR data for use in numerical weather prediction models. International Journal of Remote Sensing 1998;19(8):1543-1533.
14. Skoković D, Sobrino JA, Jimenez-Munoz JC, Soria G, Julien Y, Mattar C, Cristobal J. Calibration and validation of land surface temperature for Landsat 8-TIRS sensor. Land product Validation and Evolution, ESA/ESRIN Frascati (Italy), 2014:9-6.
15. Sobrino JA, Li ZL, Stoll MP, Becker F. Multi-channel and multi-angle algorithms for estimating sea and land surface temperature with ATSR data. International Journal of Remote Sensing 1996;17(11):2114-2089.

12/20/2017